

Multi-Parametric Sensitivity Analysis of an Electrical Potential Difference Gear Crack Sensor Using Finite Elements

Charikleia Aliberti

National Technical University of Athens, Athens, Greece

Email: caliberti@central.ntua.gr

Nikolaos Fokas and Yoon Lee

Psyche Engineering Systems and Technologies, The Hague, Netherlands

Email: rtd@psyx.eu

Abstract—In this paper a method is developed and described for the determination in real-time of the crack length at the root of a three-dimensional gear tooth of given thickness, based on the electrical potential difference method. Multi-Electrostatic analysis is carried out on multi-parametric gear solid models using finite elements, by inserting direct current from a pair of pre-attached electrodes and measuring the potential field at selected locations via other dedicated pre-attached electrode pairs and the results are correlated with the crack length. This analysis is used to determine the sensitivity of the electric sensing layout to size and other parameters, including the width of a tooth, the module, and the mounting position of the sensing electrode pairs.

Index Terms—gear teeth, crack sensor, electrical potential difference, sensitivity analysis

I. INTRODUCTION

Gears are machine components intended to transmit rotary motion and power transfer from the engine to the driven shaft via suitable cooperating teeth. The teeth are repeated recesses and protrusions of the surface of a toothed wheel, suitable to achieve meshing of the flanks of a toothed wheel with the projection of the mating gear wheel. Various curves can be used for the tooth profile, such as involute, cycloidal etc. Tooth geometry varies widely, from standard, non-standard and 3-D tooth forms [1]-[17], to entirely asymmetric tooth forms [18]-[26]. In the present study we shall consider spur gears, in which the teeth are straight, symmetric and parallel to the rotation axis of the wheel.

Most mechanical systems that include gears show sensitivity to the existing operating conditions. Irregular or adverse operating conditions, such as static or dynamically induced overloads [27]-[30], can lead to situations where the following phenomena occur:

- Development of high torque values
- Local overloading of profiles

- Improper lubrication
- Presence of foreign bodies in the partner profiles
- Insufficient maintenance on the mechanical system, such as misalignment or unbalance
- Construction error in the configuration of the gear profile
- Application improper heat treatment at gears

The operation conditions and the development of cracks on the gear due to fatigue, in combination with high rotational speeds of the mechanical system, can cause the failure or wear of the gear. This appears as:

- Root fatigue cracking
- Surface pressure fatigue (pitting)
- Adhesive Wear (scoring)

Root fatigue cracking is of particular interest in this paper, which occurs when submitting the tooth profiles to high bending stresses that exceed the material strength limit fatigue.

Such failures are classified in fracture mechanics in general as mode I (opening), II (sliding), or III (tearing).

Developing cracks at the foot of a tooth is a mixed type, namely type I and II. Consequently, there are two K_{I} and K_{II} factors characterizing the stress state of the crack in the tooth. Typically the value for K_{II} is about 10% of the value for K_{I} , which develops maximum values for middle crack lengths, with small crack lengths receiving medium values and great lengths small values. Several methods and models have been proposed over the years to detect, characterise and model gear tooth cracking, including [31]-[38] and [39]. Mainly, vibration and acoustic signature measurements are used due to the ease of instrumentation, considering that gears are difficult to access rotating systems operating under aggressive conditions and elevated temperatures, which prevail in the gearboxes.

In [39], the creation and propagation of a crack depends on the ratio $m_B = S_r/h_t$ (backup ratio), which is a function of rim thickness S_r and whole depth (h_t). For large values of the backup ratio (m_B), the crack will develop approximately as per trajectory 1 in Fig. 1,

whereas for small values of the backup ratio (m_B), it will develop as per trajectory 2.

The initial crack angle α_c constitutes one additional factor affecting crack propagation: For small α_c values the crack is not expected to propagate through the body of the tooth, even if the backup ratio is large, but instead will propagate towards the rim (Fig. 1, case B).

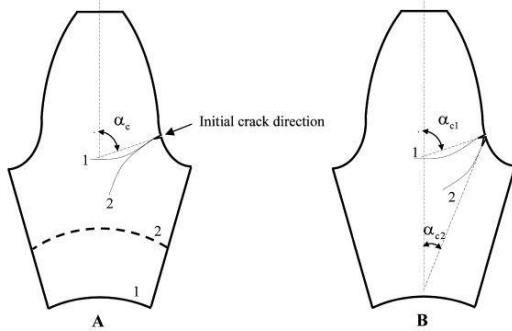


Figure 1. Influence of the backup ratio on the crack trajectory.

Moreover, the crack path tends to be a slightly curved, almost straight line [39].

Regardless of type, each machine during the operation is producing vibrations. Under ideal operating conditions, the level of vibrations is within permissible limits. In real operating conditions, any existing defects or potential harm or lead to increased levels of vibration or even the shift of the frequency spectrum.

Monitoring and analysis of vibration provides information about the condition of a machine and made through modern measuring systems and institutions. The operating principle of the measuring system is based on the signal processing principles (discrete transform Fourier (DFT), fast transformation Fourier (FFT)).

The spectra of the vibrations received by the measuring systems are characterized by peaks at frequencies corresponding to the operating periods of the engine components. In principle, the presence of a root crack will alter the stiffness of a particular tooth, thus influencing the vibration and acoustic signature and allowing an indirect inference of the existence of said crack. However, the accuracy of the methods based on this principle suffers from various strong noise sources, making the accurate characterisation of cracks impractical.

To overcome such problems direct in-situ measurements for crack detection and characterisation are needed. The electrical potential difference method presents such a possibility. It has been proven to be accurate and particularly suitable for use in inaccessible and harsh environments and elevated temperatures [40]-[59].

The potential difference method is a non-destructive detection technique applicable to electrically conductive materials. This method has two major implementation techniques [41]:

- 1) Direct current potential difference-DCPD
- 2) Alternating current potential difference-ACPD

In both techniques the basic sensing layout is as shown in Fig. 2.

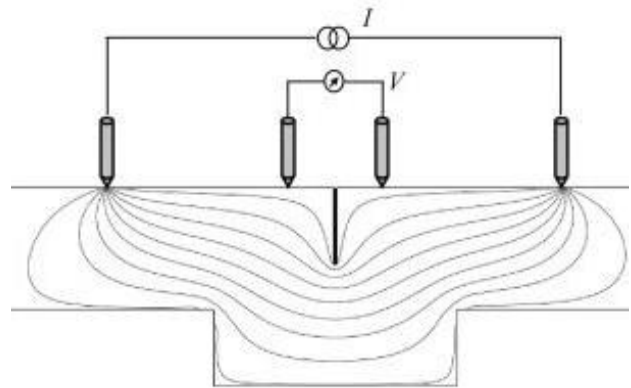


Figure 2. Placement of sensing and source/sink electrodes on both sides of a crack and current flow through the cracked body.

According to the potential difference method, electrical current is supplied (AC or DC) via electrical terminals (electrodes). The electrical current is applied to either side of the crack, resulting in the development of a potential difference at suitably located electrodes, also placed on either side of the crack. Any increase of the crack length will cause a change in electrical resistance and therefore the difference as compared to the potential difference that would be observed in a specimen without a crack.

The purpose of this work is the design of an electrical potential difference gear crack propagation sensor suitable for real-time measurement. Until today electric crack propagation sensors were analysed only in the two-dimensional plane, without taking into account the effect of the gear width.

For electrical sensor design was made using the process of the fall of electric potential, whereby positioned electrodes at suitable positions on the surface of a tooth to which imported electricity, then measure the difference in electrical potential between the other two electrodes. The information is the difference in electric potential lead to the identification of the crack length given the trajectory. The whole problem of this work focused on the path of electrical current in the body of the tooth by diffusion from the surface (electrodes) to the interior of the tooth.

II. TOOTH AND CRACK GEOMETRY AND ELECTRICAL MODEL DEFINITION

The gear geometry considered in this study has pressure angle $\alpha_0=20^\circ$ and number of teeth $Z=20$. The Highest Point of Single Tooth Contact (HPSTC) is calculated for a contact ratio ($\epsilon=1,2$). This geometry has been scaled to module values of $m=2, 3, 4, 6, 12, 24$ and $m=50$ mm. Appropriate tooth widths were assigned in each case.

A 3-D solid model for one of these gears and a single tooth model in the uncracked state is shown in Fig. 3.

To design the cracks a finite element analysis was conducted of the cantilever tooth subjected to line loading at the HPSTC, which corresponds to the most severe loading per mesh cycle in the quasi-static case. Thus the position of the highest tensile stress at the tooth root,

which is the most likely point of crack initiation, was determined.

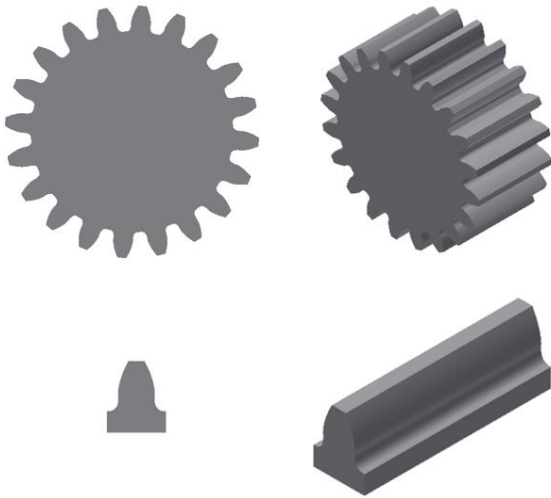


Figure 3. Uncracked gear and tooth model.

Regarding the progress of the crack, the iso-stress lines for the maximum shear stress were calculated (Fig. 4). Under the Tresca and von Mises failure criteria, the crack will propagate perpendicularly to those lines, intersecting them until it encounters the neutral axis of the tooth.

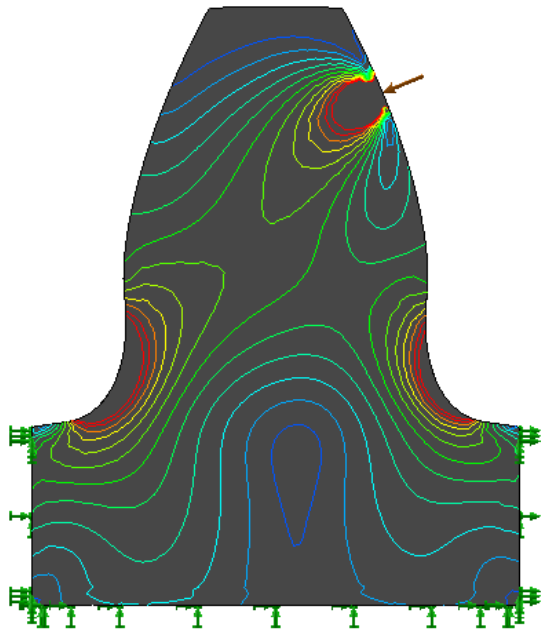


Figure 4. Iso-shear-stress lines in a gear tooth loaded at the HPSTC.

Thus anticipating the path of the crack, cracked gear model geometries are generated and imported into ANSYS Mechanical APDL. For describing crack propagation different crack tip positions are described as non-dimensional fractions of the length of a crack starting at the tooth root and ending at the tooth centre line. Specifically, the crack propagation will be discretised in ten stages, in each of which the crack will be increased by 10% compared with the previous stage, with 100% corresponding to the centre line.

In the finite element mesh the Solid 69 element was used (Fig. 5), which has two degrees of freedom at each

node, making it suitable for the intended analyses [8]. The meshed model of a cracked tooth is shown in Fig. 6.

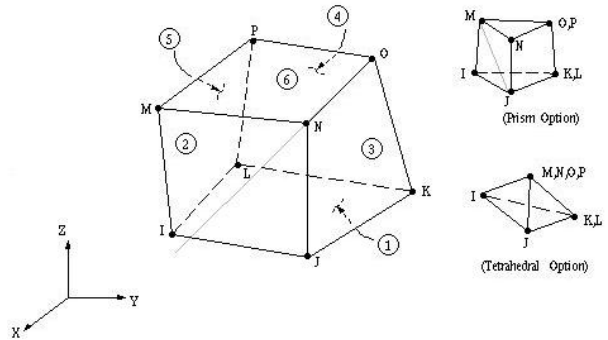


Figure 5. Definition of the Solid69 element.

The specific electrical resistance for steel was entered into the model as $\rho = 1,43 \cdot 10^{-7} \Omega\text{m}$ considering a temperature of 20 degrees Celsius. We note that:

$$\rho = \frac{E}{J} \quad (1)$$

where E is the electrical field intensity and J is the current density.

Next, several *hard points* were defined, playing the role of the electrode sources and sinks and of the electrical potential sensors.

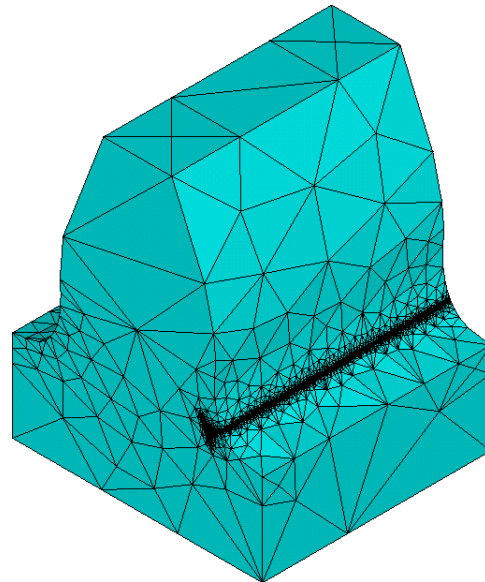


Figure 6. Finite element model of a cracked tooth with refined mesh around the crack and measurement area.

Applying constant current boundary conditions at the appropriate hard points steady state analysis may then be carried out.

III. RESULTS AND DISCUSSION

A. Effect of Width Increase

Fig. 7 shows the calculated dependence of the non-dimensional potential on the length of the crack, ranging between 10%, 20%, 30%, and 40%, and the gear width, considering very thin gears.

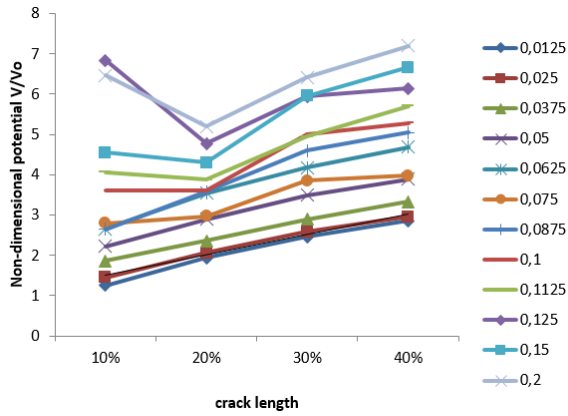


Figure 7. Dependence of the non-dimensional potential on the crack length and the tooth width.

It is observed that for very small cracks the non-dimensional potential to the crack width is nearly linear. By increasing the width beyond 0.1mm, a characteristic dip starts to become noticeable around the 20% crack length, which persists at increasing widths.

B. Current Flow Inside a Tooth with Current Injection on One Side Only

Six equidistant test sections z1-z6 are defined as per Fig. 8, with the current source and sink electrodes located on z1.

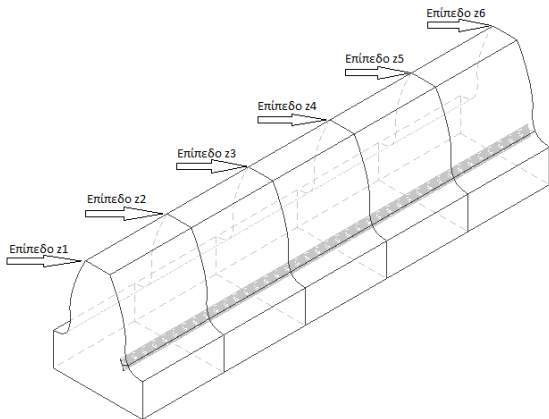


Figure 8. Definition of test sections z1-z6 on a gear tooth.

The analysis results are shown in Fig. 9.

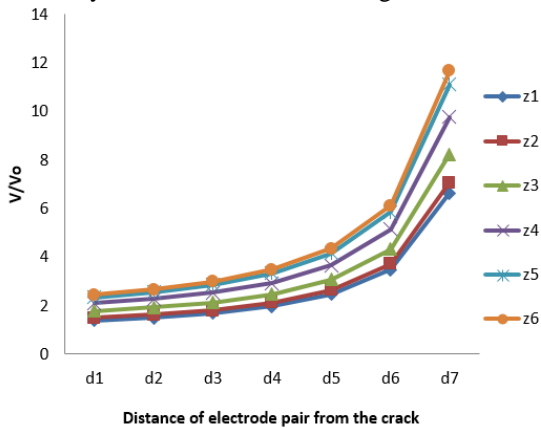


Figure 9. Non-dimensional potential at various test sections as a function of the distance of the electrode pair from the crack.

The chart reveals that the potential decreases as one moves towards the inside of the tooth. Also, for the pairs that are closest to the crack, the potential becomes larger values with respect to pairs farther removed from the crack. The 3-D current density on a plane normal to the crack tip is shown in Fig. 10.

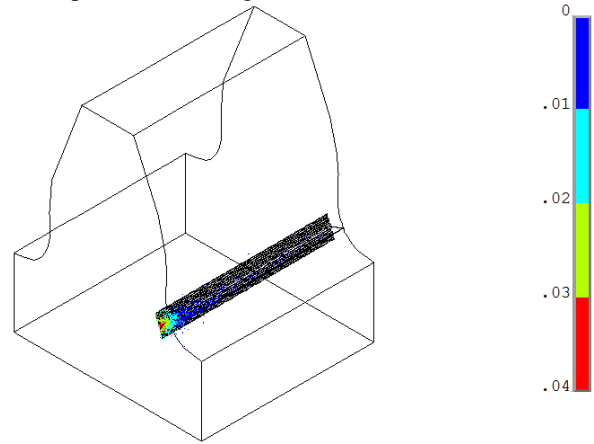


Figure 10. Current density reduction along the width of the tooth (isometric view).

C. Multi-Parametric Sensitivity Analysis

At this stage of the work a multi-parametric sensitivity analysis of the non-dimensional potential is carried out. The parameters are the crack length, the module, the width of the tooth and the distance of the pair of electrodes of the crack. The width of the crack length to be studied ranges from 10% to 40%. As regards the module, the considered values are $m = 2\text{mm}$, $m = 3\text{mm}$ and $m = 4\text{mm}$. The tooth width, expressed in terms of the module, ranges from 0.1m to 10m. Fig. 11 illustrates the influence of some parameters on the tooth form.

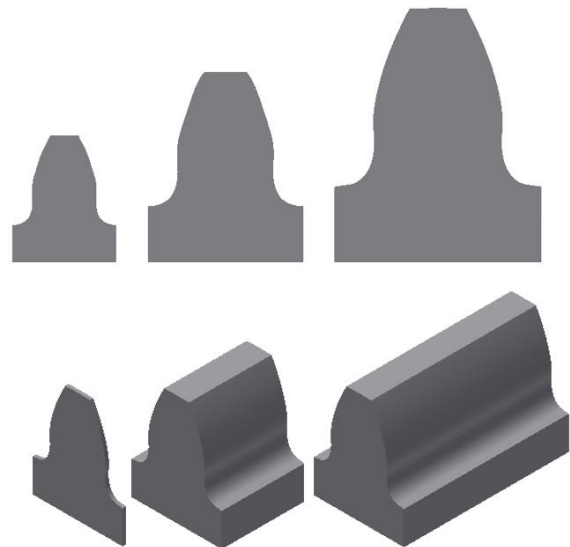


Figure 11. Top, left to right: Tooth model cross sections corresponding to module 2mm, 3mm and 4mm. Bottom, left to right: Tooth models having same module with widths of 0.1m, 2.5m and 5m.

Finally, for the distance of the electrodes from the crack, indicated that seven pairs of electrodes are controlled in five partitions per width of each tooth. Thus

created in total $7 \times 6 \times 2 = 84$ hardpoints (42 pairs of hardpoints) for each phase of the crack (10%, 20%, 30%, 40%) and respectively each tooth. These pairs are always placed marginally shortly before the end of the crack.

The simulation results are summarised in Fig. 12-Fig. 13.

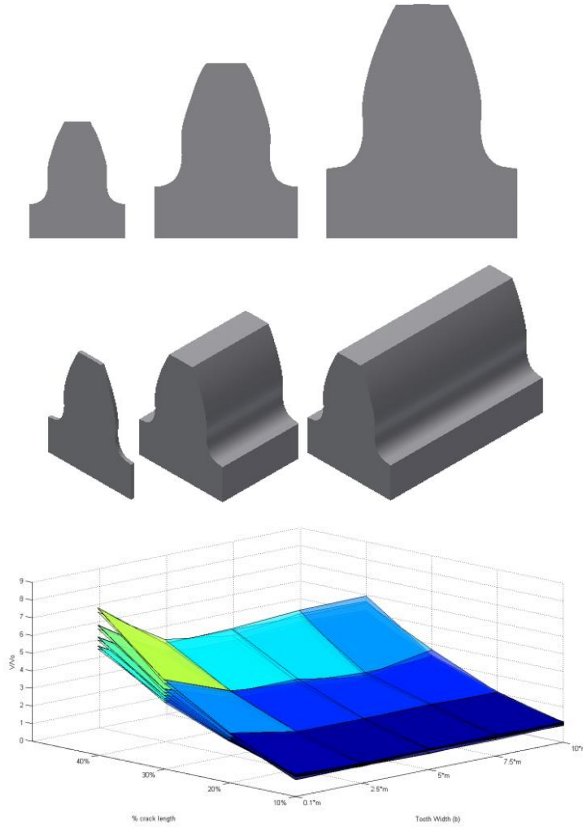


Figure 12. Non-dimensional potential V/V_0 , having as parameter the distance of the electrodes from the crack.

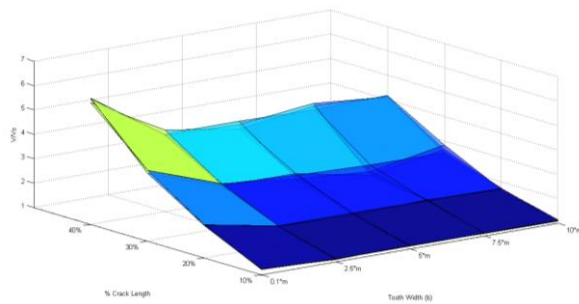


Figure 13. Non-dimensional potential V/V_0 , having as parameter the module $m=2, m=3, m=4$.

From Fig. 12-Fig. 13 it is concluded that the width of a tooth does not significantly affect the non-dimensional potential, except in the case of very small tooth widths (0,1m), in which case there is an increase in the non-dimensional potential. The module of one tooth, at least for the range studied ($m=2$ up to $m=4$), does not affect the value of the non-dimensional potential. In contrast, the development of the crack from 10% to 40%, the potential almost linearly affects it. Regarding the pairs of potential measuring electrodes, it is observed that the smaller the distance from the crack, the more increased the potential

value recorded. Consequently, it is best to place the electrodes as close to the crack as possible; however, there is the caveat that the actual crack position cannot be predicted a priori, so a minimal distance must be observed during electrode placement to account for this uncertainty.

IV. CONCLUSIONS

In this paper a multi parametric electrical model of cracked gear teeth was developed and simulated and the dependency and sensitivity was established of non-dimensional electrical potential measurements using a specially developed electrode configuration. In particular, the dependency of practical surface measurements on the tooth width was found to be strong only for small tooth widths, quickly vanishing at larger practically applied widths. No dependency on the gear size factor (module) was observed. Useful correlations were observed between the crack depth and the electrical potential, establishing that this method is practically applicable in principle to gears of all sizes and proportions. The sensitivity to the placement of electrodes, in terms of distance from the crack, was also established.

REFERENCES

- [1] F. L. Litvin, A. G. Wang, and R. F. Handschuh, "Computerized generation and simulation of meshing and contact of spiral bevel gears with improved geometry," *Computer Methods in Applied Mechanics and Engineering*, vol. 158, no. 1-2, pp. 35-64, 1998.
- [2] F. L. Litvin, A. G. Wang, and R. F. Handschuh, "Computerized design and analysis of face-milled, uniform tooth height spiral bevel gear drives," *J. Mech. Des.*, vol. 118, pp. 573-579, 1996.
- [3] Y. Zhang, F. L. Litvin, and R. F. Handschuh, "Computerized design of low-noise face-milled spiral bevel gears," *Mech. Mach. Theory*, vol. 30, no. 8, pp. 1171-1178, 1995.
- [4] C. Spitas, V. Spitas, A. Amani, and M. Rajabalinejad, "Parametric investigation of the combined effect of whole depth and cutter tip radius on the bending strength of 20° involute gear teeth," *Acta Mechanica*, vol. 225, no. 2, pp. 361-371, 2014.
- [5] V. Spitas and C. Spitas, "Numerical and experimental comparative study of strength-optimised AGMA and FZG spur gears," *Acta Mechanica*, vol. 193, no. 1-2, pp. 113-126, 2007.
- [6] F. L. Litvin and Y. Zhang, "Local synthesis and tooth contact analysis of face-milled spiral bevel gears," NASA Contractor Report 4342, AVSCOM Technical Report 90-C-028, 1991.
- [7] F. L. Litvin, P. Rahman, and R. N. Goldrich, "Mathematical models for the synthesis and optimization of spiral bevel gear tooth surfaces," NASA CR-3553, 1982.
- [8] F. L. Litvin, A. Fuentes, C. Zanzi, P. Matteo, and F. R. Handschuh, "Design, generation and stress analysis of two versions of geometry of face-gear drives," *Mech. Machine Theory*, vol. 37, pp. 1179-1211, 2002.
- [9] V. Spitas and C. Spitas, "Four-parametric design study of the bending strength of circular-fillet vs. trochoidal-fillet in gear tooth design using BEM," *Mechanics Based Design of Structures and Machines*, vol. 35, no. 2, pp. 163-178, 2007.
- [10] C. Spitas and V. Spitas, "A FEM study of the bending strength of circular fillet gear teeth compared to trochoidal fillets produced with enlarged cutter tip radius," *Mechanics Based Design of Structures and Machines*, vol. 35, no. 1, pp. 59-73, 2007.
- [11] F. L. Litvin, J. C. Wang, Y. J. D. Chen, R. B. Bossler, G. F. Heath, and D. J. Lewicki, "Face-gear drives: Design, analysis and testing for helicopter transmission applications," AGMA Paper 92FTM2, 1992.
- [12] V. Spitas and C. Spitas, "Optimising involute gear design for maximum bending strength and equivalent pitting resistance," *Journal of Mechanical Engineering Science*, vol. 221, pp. 479-488, 2006.

- [13] V. Spitas, T. Costopoulos, and C. Spitas, "Optimum gear tooth geometry for minimum fillet stress using BEM and experimental verification with photoelasticity," *Journal of Mechanical Design*, vol. 128, no. 5, pp. 1159-1164, 2006.
- [14] J. Wang and I. Howard, "Finite element analysis of high contact ratio spur gears in mesh," *Journal of Tribology*, vol. 127, no. 3, pp. 469-483, 2005.
- [15] C. Spitas and V. Spitas, "Generating standard 20° involute pinions with increased fillet strength by using 25° rack cutters with non-standard module," *Journal of Mechanical Engineering Science*, vol. 220, no. 8, pp. 1297-1304, 2006.
- [16] C. Spitas and V. Spitas, "Can non-standard involute gears of different modules mesh?" *Journal of Mechanical Engineering Science*, vol. 220, no. 8, pp. 1305-1313, 2006.
- [17] C. Lee, H. H. Lin, F. B. Oswald, and D. P. Townsend, "Influence of linear profile modification and loading conditions on the dynamic tooth load and stress of high-contact-ratio spur gears," *J. Mech. Des.*, vol. 113, no. 4, pp. 473-480, 1991.
- [18] F. L. Litvin, Q. Lian, and A. L. Kapelevich, "Asymmetric modified gear drives: reduction of noise, localization of contact, simulation of meshing and stress analysis," *Comput. Meth. Appl. Mech. Eng.*, vol. 188, no. 1, pp. 363-390, 2000.
- [19] A. L. Kapelevich and R. E. Kleiss, "Direct gear design for spur and helical involute gears," *Gear Technol.*, vol. 19, no. 5, pp. 29-35, 2002.
- [20] A. Kapelevich and Y. V. Shekhtman, "Direct gear design: Bending stress minimization," *Gear Technol.*, vol. 20, no. 5, pp. 44-47, 2003.
- [21] V. Spitas, C. Spitas, and T. Costopoulos, "Reduction of tooth fillet stresses using novel one-sided involute asymmetric gear design," *Mechanics Based Design of Structures and Machines*, vol. 37, no. 2, pp. 157-182, 2009.
- [22] G. Deng, T. Nakanishi, and K. Inoue, "Bending load capacity enhancement using an asymmetric tooth profile," *JSME Int. J.*, vol. 46, pp. 1171-1176, 2003.
- [23] K. Cavdar, F. Karpat, and F. C. Babalik, "Computer aided analysis of bending strength of involute spur gears with asymmetric profile," *ASME J. Mech. Des.*, vol. 127, pp. 477-484, 2005.
- [24] S. C. Yang, "Mathematical model of a helical gear with asymmetric involute teeth and its analysis," *Int. J. Adv. Manufact. Technol.*, vol. 26, pp. 448-456, 2005.
- [25] D. V. Muni, V. Senthilkumar, and G. Muthuveerappan, "Optimization of asymmetric spur gear drives for maximum bending strength using direct gear design method," *Mech. Based Des. Struct. Mach.*, vol. 35, pp. 127-145, 2007.
- [26] A. Kapelevich, "Geometry and design of involute spur gears with asymmetric teeth," *Mech. Mach. Theory*, vol. 35, pp. 117-130, 2000.
- [27] S. L. T. de Souza, I. L. Caldas, R. L. Viana, and J. M. Balthazar, "Sudden changes in chaotic attractors and transient basins in a model for rattling in gearboxes," *Chaos, Solitons & Fractals*, vol. 21, no. 3, pp. 763-772, 2004.
- [28] C. Spitas and V. Spitas, "Coupled Multi-DOF dynamic contact analysis model for the simulation of intermittent gear tooth contacts, impacts and rattling considering backlash and variable torque," *Journal of Mechanical Engineering Science*, vol. 230, no. 7-8, pp. 1022-1047, 2015.
- [29] C. Spitas and V. Spitas, "Calculation of overloads induced by indexing errors in spur gearboxes using multi-degree-of-freedom dynamical simulation," *IMECE Journal of Multi-Body Dynamics*, vol. 220, no. 4, pp. 273-282, 2006.
- [30] M. Franulovic, R. Basan, R. Kunc, and I. Prebil, "Numerical modelling of fatigue damage in gears tooth root," *ICMFF9*, 2013.
- [31] J. J. Zakrajsek, R. F. Handschuh, D. G. Lewicki, and H. J. Decker, "Detecting gear tooth fracture in a high contact ratio face gear mesh," Technical Memorandum, ADA298645, 1995.
- [32] W. Wang, "Early detection of gear tooth cracking using the resonance demodulation technique," *Mechanical Systems and Signal Processing*, vol. 15, no. 5, pp. 887-903, 2001.
- [33] P. D. McFadden, "Detecting fatigue cracks in gears by amplitude and phase demodulation of the meshing vibration," *Journal of Vibration, Acoustics, Stress, and Reliability in Design*, vol. 108, pp. 165-170, 1986.
- [34] F. K. Choy, et al., "Vibration signature analysis of a faulted gear transmission system," NASA Technical Memorandum 106623, 1994.
- [35] T. Barszcz and R. B. Randall, "Application of spectral kurtosis for detection of a tooth crack in the planetary gear of a wind turbine," *Mechanical Systems and Signal Processing*, vol. 23, no. 4, pp. 1352-1365, 2009.
- [36] W. J. Wang and P. D. McFadden, "Decomposition of gear motion signals and its application to gearbox diagnostics," *Journal of Vibration and Acoustics*, vol. 117, pp. 363-369, 1995.
- [37] W. Wang, F. Ismail, and M. F. Golnaraghi, "Assessment of gear damage monitoring techniques using vibration measurements," *Mechanical Systems and Signal Processing*, vol. 15, pp. 905-922, 2001.
- [38] D. Lin, M. Wisenman, D. Banjevic, A. K. S. Andrew, and S. Jardine, "An approach to signal processing and condition-based maintenance for gearboxes subject to tooth failure," *Mechanical Systems and Signal Processing*, vol. 18, pp. 993-1007, 2004.
- [39] F. Chaari, T. Fakhfakh, and M. Haddar, "Analytical modelling of spur gear tooth crack and influence on gearmesh stiffness," *European Journal of Mechanics-A/Solids*, vol. 28, no. 3, pp. 461-468, 2009.
- [40] V. Spitas, C. Spitas, and P. Michelis, "A three-point electrical potential difference method for in situ monitoring of propagating mixed-mode cracks at high temperature," *Measurement*, vol. 43, no. 7, pp. 950-959, 2010.
- [41] V. Spitas, C. Spitas, and P. Michelis, "Real-time measurement of shear fatigue crack propagation at high-temperature using the potential drop technique," *Measurement*, vol. 41, no. 4, pp. 424-432, 2008.
- [42] W. D. Dover and L. J. Bond, "Weld crack characterization on offshore structures using AC potential difference and ultrasonics," *NDT international*, vol. 19, no. 4, pp. 243-247, 1984.
- [43] M. Andersson, C. Persson, and S. Melin, "Experimental and numerical investigation of crack closure measurements with electrical potential drop technique," *Int. J. Fatigue*, pp. 1059-1068, 2006.
- [44] V. Spitas and P. Michelis, "The potential drop technique for measuring crack growth in shear," *Fracture of Nano and Engineering Materials and Structures*, Springer, pp. 463-464, 2006.
- [45] Y. Sato, N. Kawaguchi, N. Ogura, and T. Kitayama, "Automated visualization of surface morphology of cracks by means of induced current potential drop technique," *NDT&E Int.*, pp. 83-89, 2012.
- [46] R. Ghajar, "An alternative method for crack interaction in NDE of multiple cracks by means of potential drop technique," *NDT&E Int.*, pp. 539-544, 2004.
- [47] I. Cerny, "Measurement of subcritical growth of defects in large components of nuclear power plants at elevated temperatures," *Eng Fract Mech*, vol. 71, pp. 837-848, 2001.
- [48] G. H. Aronson and R. O. Ritchie, "Optimization of the electrical potential technique for crack growth monitoring in compact test pieces using finite element analysis," *J. Test Eval.*, pp. 208-214, 1979.
- [49] I. Cerny, "Growth and retardation of physically short fatigue cracks in an aircraft Al-alloy after shot peening," *Procedia Eng*, vol. 10, pp. 3411-3416, 2011.
- [50] L. Doremus, Y. Nadot, G. Henaff, C. Mary, and S. Pierret, "Calibration of the potential drop method for monitoring small crack growth from surface anomalies - Crack front marking technique and finite element simulations," *International Journal of Fatigue*, vol. 70, pp. 178-185, 2015.
- [51] M. A. Hicks and A. C. Pickard, "A comparison of theoretical and experimental methods of calibrating the electrical potential drop technique for crack length determination," *Int. J. Fract.*, vol. 20, no. 2, pp. 91-101, 1982.
- [52] I. Cerny, "The use of DCPD method for measurement of growth of cracks in large components at normal and elevated temperatures," *Eng. Fract Mech.*, vol. 71, pp. 837-848, 2004.
- [53] D. A. Green, J. M. Kendall, and J. F. Knott, "Analytic and analogue techniques for determining potential distributions around angled cracks," *Int. J. Fract.*, vol. 37, pp. R3-R12, 1988.
- [54] J. A. Joyce and C. S. Schneider, "Crack length measurement during rapid crack growth using an alternating-current potential difference method," *J. Test Eval.*, vol. 16, no. 3, pp. 257-270, 1988.
- [55] V. Spitas, M. Besterci, P. Michelis, and C. Spitas, "Shear testing of Al and Al-Al4C3 materials at elevated temperatures," *High*

Temperature Materials and Processes, vol. 24, no. 3, pp. 145-152, 2005.

- [56] R. Pilkington, D. Hutchinson, and C. L. Jones, "High-temperature crack-opening displacement measurements in a ferritic steel," *Metal Science*, vol. 8, no. 1, pp. 237-241, 2013.
- [57] L. Gandossi, S. A. Summers, N. G. Taylor, R. C. Hurst, B. J. Hulm, and J. D. Parker, "The potential drop method for monitoring crack growth in real components subjected to combined fatigue and creep conditions: Application of FE techniques for deriving calibration curves," *Int. J. Press Vessels Pip*, pp. 881-891, 2001.
- [58] C. Ennaceur, A. Laksimi, C. Hervé and M. Cherfaoui, "Monitoring crack growth in pressure vessel steels by the acoustic emission technique and the method of potential difference," *International Journal of Pressure Vessels and Piping*, vol. 83, no. 3, pp. 197-204, 2006.
- [59] G. A. Schneider, F. Felten, and R. M. McMeeking, "The electrical potential difference across cracks in PZT measured by Kelvin

Probe Microscopy and the implications for fracture," *Acta materialia*, vol. 51, no. 8, pp. 2235-2241, 2003.

Charikleia Aliberti holds a Diploma in mechanical engineering from the National Technical University of Athens. Her diploma thesis was on the NDT of machine elements using the DCPD technique.

Nikolaos Fokas holds a MSc in Mechanical Engineering with a specialisation in Machine Design. He is a senior engineer at Psyche Engineering Systems and Technologies BV and is involved in the R&D of high performance mechanical powertrains, with particular focus on efficiency, compactness and reliability.

Yoon Lee is a BSc in mechatronics engineering at Psyche Engineering Systems and Technologies BV. His expertise lies in technical instrumentation, measurement and control.